Electrochimica Acta 214 (2016) 326–335

Contents lists available at ScienceDirect

Electrochimica Acta

journal homepage: www.elsevier.com/locate/electacta

Monolithic Porous Magnéli-phase Ti_4O_7 for Electro-oxidation Treatment of Industrial Wastewater

Shijie You[a,*], Bo Liu[a], Yifan Gao[a], Yu Wang[a], Chuyang Y. Tang[b,**], Yibing Huang[c], Nanqi Ren[a]

[a] State Key Laboratory of Urban Water Resource and Environment, Harbin Institute of Technology, Harbin 150090, PR China
[b] Department of Civil Engineering, The University of Hong Kong, HW6-19B, Haking Wong Building, Pokfulam, Hong Kong
[c] Ti-Dynamics Company Limited, Changsha 410005, PR China

ARTICLE INFO

Article history:
Received 8 June 2016
Received in revised form 8 August 2016
Accepted 8 August 2016
Available online 9 August 2016

Keywords:
Magnéli-phase Ti_4O_7 electrode
Electrochemical oxidation
Dyeing and finishing wastewater

ABSTRACT

Electrochemical oxidation (EO) processes have been gaining a growing popularity in wastewater treatment. Their engineered applications inspire the search for conductive, stable, inexpensive, and sustainable electrode materials. Magnéli-phase titanium oxides have unique crystal and electron structure, which result in good electrical conductivity approaching that of metal and excellent corrosion resistance close to that of ceramics. We fabricated a monolithic porous Magnéli-phase Ti_4O_7 electrode for EO of refractory industrial dyeing and finishing wastewater (DFWW). The results demonstrated that the electrochemically active area of porous Ti_4O_7 electrode was 2–3 orders of magnitude higher than the apparent surface area of bulk electrode. The Ti_4O_7 electrode achieved efficient and stable abatement of recalcitrant organic pollutants on site without any extra addition of chemicals. The soluble chemical oxygen demand (COD) and dissolved organic carbon (DOC) were removed by 66.5% and 46.7%, respectively, at current density of 8 mA cm^{-2} after 2 h reaction. The bioavailability of treated wastewater was improved substantially, indicated by one order of magnitude increase in BOD_5/COD. The Ti_4O_7 electrode had good long-term stability, with its maximum COD removal declined only slightly (<8%) at current density of 20 mA cm^{-2} during a 50-cycle operation. The organic pollutants appear most likely to be oxidized by electrochemically generated active species like physisorbed $^{\bullet}OH$ radical and aqueous ClO^- species under mass transfer control condition. The current study provides important insights for achieving efficient and sustainable electrochemical wastewater treatment using the novel porous Ti_4O_7 electrode material.

1. Introduction

Recently, tremendous potential offered by electrochemistry has been realized in a broad range of applications for water and wastewater treatment. Electrochemical oxidation (EO) that accomplishes organic degradation by direct or indirect oxidation has become competitive for water and wastewater treatment by its virtue of high efficiency, simplicity, sustainability, and ease of manipulation. [1] However, there remain several aspects of EO that need further investigation if the engineered applications are to be better implemented and developed. Over a long period, there exists a dilemma for electrode material, among the electrical conductivity, electrochemical activity, chemical stability, economic reliability and environmental availability. For example, the electrodes based on doped-SnO_2 and PbO_2 are widely adopted, but highly toxic antimony is often required as agent for doping SnO_2 [2]. Likewise, PbO_2 has been also used with very limited success due to the leaching of toxic lead into solution at anodic polarization condition [3,4]. Although boron-doping diamond (BDD) has been regarded as the most promising candidate [5–8], the large surface area is necessary to match the capability of scale-up wastewater treatment, which adds the capital cost substantially. As such, these inconsistencies have been creating an incentive to explore an "ideal" electrode material for scale-up EO process.

Titanium dioxide (TiO_2) is a well-known semi-conductor which has been widely used in photocatalytic reactions. Interestingly, the electronic properties of TiO_2 can be drastically transformed by establishing oxygen deficiencies within the crystalline lattice,

* Corresponding author at: P.O. Box 2603#, No. 73, Huanghe Road, Nangang District, Harbin, 150090, China.
** Corresponding author.
E-mail addresses: sjyou@hit.edu.cn (S. You), tangc@hku.hk (C.Y. Tang).

http://dx.doi.org/10.1016/j.electacta.2016.08.037
0013-4686/

giving rise to what is called Magnéli-phase titanium oxides with a generic formula of Ti_xO_{2x-1} ($4 \le x \le 10$) [9]. Magnéli-phase titanium oxides have a crystal structure of oxygen deficiency for every *x*th layer, resulting in the shear planes where 2D chains of octahedra become face sharing to accommodate the deficiency in oxygen. This unique structure leads to a combination of outstanding electrical conductivity approaching to that of metals and great corrosion resistance close to that of ceramic materials [10]. For example, Ti_4O_7 ($x = 4$, under trade name Ebonex®, Atraverda Ltd, U.K.) exhibits a great conductivity of $\sim$1000 S cm^{-1}, which is even higher than that of graphitic carbon ($\sim$727 S cm^{-1}) [11]. Additionally, Ti_4O_7 can also offer higher oxygen evolution potential (+2.6 V vs standard hydrogen electrode, SHE) than BDD. These properties make Ti_4O_7 suitable for many electrochemical applications, such as cathodic protection [12], bipolar battery [13], water spiltting [14], as well as water treatment [15–17].

Most of lab-scale EO experiments used synthetic pollutant and added high-concentration salt as background electrolyte to increase ionic conductivity, giving a concentration much higher than those existed in realistic wastewater. From an engineered point of view, however, this is far from a real scenario where the nature and concentration of pollutants and salts are determined by the industrial processes they are produced. The dyeing and finishing wastewater (DFWW) is commonly characterized to have an extremely complex composition, some of which persisting in the environment may cause severe physiological toxicity once they end up in the food chain (web) and human body. Generally, the total chemical oxygen demand (COD) can be decreased by nearly 70–80% following physicochemical primary treatments (*e.g.* coagulation, flocculation, and sedimentation) and secondary biological process [18]. Nonetheless, owing to the existence of biorefractory organic matters, the residual COD remains high in the effluent, making it not always meet the legal discharge limit [19]. Thus, the tertiary treatment is imperative before the wastewater can be discharged into receiving water bodies. It is noticed that the DFWW contains high-concentration chloride and high ionic conductivity, which makes it inherently suitable to electrochemical system. In the EO process, the porous structure of electrode is preferred because it can provide larger surface area and active sites. Besides, the protons produced from water oxidation can maintain a much lower local pH in the porous apertures than in bulk solution, which is favorable for the formation of active chlorine [20–23], an effective oxidant for organic decomposition.

Herein, we make an attempt to fabricate monolithic porous Magnéli-phase Ti_4O_7 as anode for EO of industrial DFWW. Following characterization of morphology, crystal, and surface area, the electrochemical properties of Ti_4O_7 were investigated, including the porosity and electrochemically active area, electrochemistry impedance spectroscopy, Tafel behavior and accelerated lifetime tests. Thereafter, the EO performances of monolithic Ti_4O_7 was examined and assessed for removing organic pollutants in DFWW. Last, possible mechanisms of electrochemical process of Ti_4O_7 were analyzed and discussed.

2. Materials and methods

All the chemicals used were of analytical reagents grade. Unless stated otherwise, all the experiments were done at room temperature (25 °C) and 1.0 atm pressure.

2.1. Fabrication of Monolithic Porous Ti_4O_7 Electrode

The monolithic porous Ti_4O_7, produced from high-temperature reduction of TiO_2 by H_2 was supplied by Ti-Dynamics Co. Ltd. (China). In brief, rutile TiO_2 powders were mixed by water and isopropanol (1:1, v/v) to decrease the capillary force of powder, followed by drying and addition of a 5% (w/w) polyethylene oxide binder. The mixture was compressed at 20 MPa to form a plate shape (4 cm × 4 cm × 1 cm). The plate blocks were sintered in air at a temperature of 1050 °C for 24 h, and then transferred into a furnace for reduction at H_2 atmosphere at 1050 °C for 4 h in the presence of carbon as porosity-producing agent.

2.2. Characterization

The morphology of the Ti_4O_7 electrode was observed by using field-emission scanning electron microscopy (SEM, Helios Nanolab600i, FEI, U.S.). The powder X-ray diffraction (XRD) analysis was conducted on an X-ray diffractometer (Bruke D8 Adv., Germany) and using Cu Kα radiation (λ = 0.15406 nm) at a power of 40 KeV × 30 mA. The BET surface areas were calculated based on the adsorption and desorption branches measured by using accelerated surface area and Porosometry system (ASAP 2020, Global Spec. Inc., U.S.).

The electrochemical measurements of Ti_4O_7 electrode were tested by making a comparison with widely used graphite plate (4 cm × 4 cm × 1 cm) upon PARSTAT electrochemical workstation (CHI 750D, Chenhua Co. Ltd., China). The experiments were conducted in Na_2SO_4 electrolyte (0.5 mol L^{-1}) with monolithic Ti_4O_7 as working electrode (WE), Pt sheet as counter electrode (CE, 1.0 cm^2) and Ag/AgCl (+0.197 V vs standard hydrogen electrode, SHE) as reference electrode (RE), respectively. Unless stated otherwise, all the potentials were reported with reference to Ag/AgCl electrode. For the electrochemistry impedance spectroscopy (EIS) analysis, a sine wave with frequency ranging from 10^5 to 10^{-2} Hz on the top of bias potentials was applied. The accelerated life tests were performed by recording potential versus time at constant current density of 10^3 mA cm^{-2} in 3 mol L^{-1} H_2SO_4 at 30 °C, according to the procedures described previously [24].

2.3. Dyeing and Finishing Wastewater

The dyeing and finishing wastewater (DFWW) was collected from the effluent of the sedimentation tank of Linjiang Wastewater Treatment Plant (WWTP) in Xiaoshan District, Hangzhou City. The WWTP was designed with a capacity of approximately 300,000 m^3 d^{-1} and treating process of bio-sorption, anaerobic hydrolysis, aerobic oxidation, and secondary sedimentation. The treated effluent contained soluble chemical oxygen demand (COD) of 183 mg L^{-1}, dissolved organic carbon (DOC) of 108 mg L^{-1}, and chloride ions of 1042 mg L^{-1} (conductivity of 6640 μS cm^{-1}). The low BOD_5/COD (0.029) indicated biorefractory nature of the organic pollutants. Table S1 summarized the quality of DFWW in detail.

2.4. Experimental Setup and Procedures

EO of DFWW was carried out under batch mode in a glass beaker at stirring condition (800 rpm). The anode, *i.e.* monolithic Ti_4O_7, was partially immersed into 100 mL wastewater, giving 20-cm^2 geometric area in contact with wastewater. The stainless steel plate was employed as cathode (20 cm^2). The electrode spacing was kept 10 cm. The alligator clips were used for ohmic connection of electrode and external circuit. The EO experiments were conducted at galvanostatic condition by stepwise change of current from 40 mA (2 mA cm^{-2}) to 600 mA (30 mA cm^{-2}) using a DC-regulated power supply (0–30 V and 0–3 A; TeKPower, China). The wastewater samples were collected periodically at predetermined time intervals (0.5 h, 1.0 h, 2.0 h, and 3.0 h) for COD, DOC, and pH measurements. The experiments for detecting electrogenerated active species (*i. e.* •OH radicals and active chlorines) by Ti_4O_7 were performed based on the electrolysis of NaCl solution

(1000 mg L^{-1}, pH 8.3) at current density of 2 mA cm^{-2} and 20 mA cm^{-2}, respectively.

2.5. Analyses and Calculations

The wastewater samples were first filtered through a 0.2-μm acetate fibrous membrane to remove particulate impurities, and then soluble chemical oxygen demand (COD) and five-day biochemical oxygen demand (BOD_5) were determined by using standard methods [25]. The dissolved organic carbon (DOC) was analyzed by using total organic carbon (TOC) analyzer (Shimadzu, VSCN8, Japan). The pH was measured by using a pH meter (type pHs-3c, Leici, China). The molecules of different organic pollutants were analyzed qualitatively by using high-performance liquid chromatography with electrospray ionization mass spectrometry (HPLC-ESI/MS, Agilent 6460, U.S.) on the basis of their mass/charge ratio (m/z). The free and total chlorine was determined using N,N-diethyl-p-phenylendiamine methods based on colorimeter (type DR/890, Hach, U.S.). The •OH radicals were detected with 5,5-Dimethyl-1-pyrroline N-oxide (DMPO) serving as spin-trapping agent using electron paramagnetic resonance (EPR, Bruker, Germany).

The current efficiency (CE), instantaneous current efficiency (ICE) and energy consumption (W) were calculated according to

$$CE(\%) = \frac{\Delta \mathrm{sCOD} bFV}{M_{O2} It} \quad (1)$$

$$ICE(\%) = \frac{[\mathrm{sCOD}(t) - \mathrm{sCOD}(t+\Delta t)]bFV}{M_{O2} I \Delta t} \quad (2)$$

$$W\,(\mathrm{kWh\ m^{-3}}) = \frac{\Delta E I t}{V} \quad (3)$$

where ΔCOD (mg L^{-1}) is the COD removed within reaction time of t (s), COD(t) and COD($t+\Delta t$) the COD at time t and $t+\Delta t$, b (4) the number of electron transfer, F (96485C mol^{-1}) the Faraday constant, V (m^3) the volume of wastewater, M_{O2} (32 g mol^{-1}) the relative molecular mass of oxygen, I (A) the applied current, and ΔE (V) the corresponding average voltage.

3. Results and discussion

3.1. Electrode Characterization

The XRD profiles (Fig. 1A) were indexed to the characteristic peaks of Ti_4O_7 according to reference spectrum (JCPDS No. 500787) and prior literatures, [26] revealing the evolution from TiO_2 to Ti_4O_7 originating from the rearrangement of lattice derived from oxygen release during thermal reduction by H_2. [27] Residual rutile TiO_2 was also present, as revealed by the characteristic peaks of $2\theta \approx 27.5°$ (JCPDS No. 761940). Fig. 1B and C provide the apparent and micro surface morphology of monolithic porous Ti_4O_7,

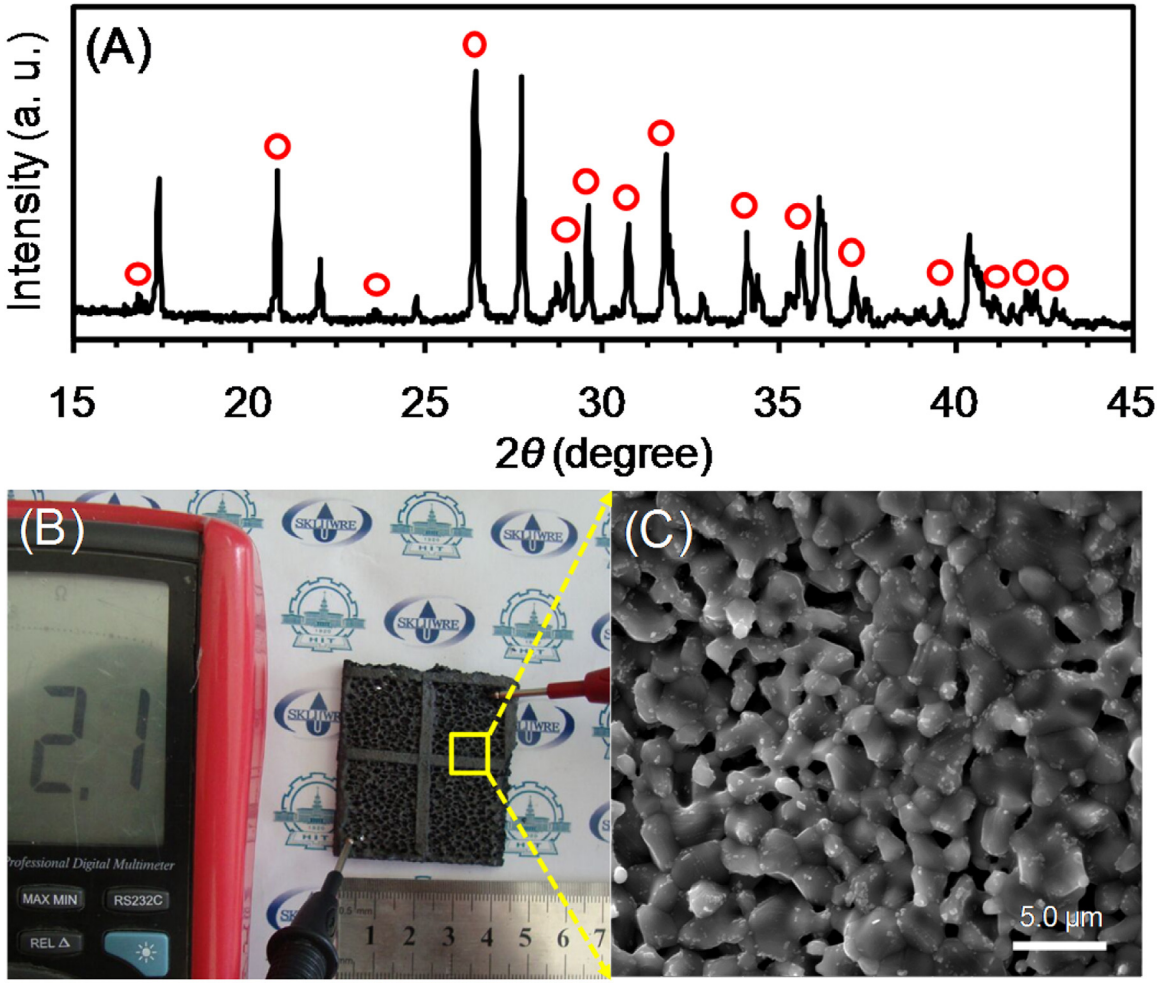

Fig. 1. (A) XRD profiles, (B) optical image and (C) SEM observation of as-prepared monolithic porous Ti_4O_7 electrode.

showing that the electrode was made of uniformly-sized particles of approximately 1.0-2.0 μm. Following high-temperature sintering process, the agglomerates of solid particles and particle-particle bonding result in the formation of porous structure inside the cavity in the presence of porosity-producing agent. The electrode surface area of approximately 0.19 $m^2 g^{-1}$ (Fig. S1) and macro porous structure will be expected beneficial for facilitating interfacial mass transfer during electrochemical reaction.

3.2. Electrochemical Properties

The resistance of monolithic Ti_4O_7 was measured to be 2.1 Ω (0.37 Ω cm^{-1}), which was an indicative of high electrical conductivity (Fig. 1B). Thereafter, to investigate the dependence of electrochemically active area on porosity of Ti_4O_7 electrode, the cyclic voltammograms (CV) measurement was performed at potential between oxygen and hydrogen evolution (*i.e.* −0.4–1.0 V vs Ag/AgCl) and sweep rate of 1–30 mV s^{-1}. As shown in Fig. 2, the Ti_4O_7 exhibited obvious capacitive behavior, and the capacitive current increased linearly with the increase in sweep rate. Accordingly, the slope of current-sweep rate line (inserted) gave the differential capacitance of the electrode/solution interface according to

$$C_{\text{Interface}} = \frac{j(\text{mA cm}^{-2})}{dE/dt(\text{mV s}^{-1})} = 3 \times 10^{-2}\text{F cm}^{-2} \quad (4)$$

If the double-layer capacitance of the metal oxide surface is assumed to be $C_0 = 6 \times 10^{-5}$ F cm^{-2} [28], the roughness factor (τ) can be estimated as

$$\tau = \frac{C_{\text{Interface}}}{C_0} = \frac{3 \times 10^{-2}\text{F cm}^{-2}}{6 \times 10^{-5}\text{F cm}^{-2}} = 500 \quad (5)$$

That is, the electrochemically active area (*i.e.* the roughness factor τ) of porous Ti_4O_7 electrode is 2–3 orders of magnitude higher than the apparent surface area of bulk electrode, revealing the important role of porous structure of electrode in providing larger electrochemically active area. This result is consistent with greater surface area measured by Porosometry analysis.

A stepwise increase in potential was implemented by recording current response to show water oxidation potential in the Na_2SO_4 electrolyte (Fig. 3A and Fig. S2). For Ti_4O_7, there was a negligible response of current when the potential was below 2.0 V. Further increasing potential resulted in an apparent enhancement of current, indicating the potential for water oxidation should be within the range of 2.0–2.5 V. This result was comparable with that of oxygen evolution potential as high as 2.5 V reported by Smith et al. [29] The same analysis gave a much lower water oxidation potential (1.2–1.5 V) for graphite plate electrode.

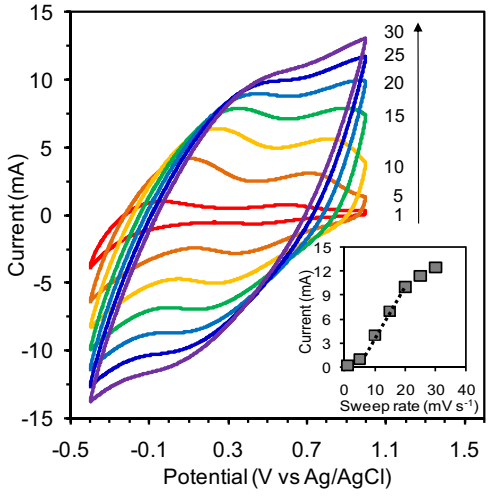

Fig. 2. Cyclic voltammogram (CV) curves for monolithic Ti_4O_7 in 0.5 mol L^{-1} Na_2SO_4 solution at sweep rate ranging from 1 mV s^{-1} to 30 mV s^{-1}. The inserted figure shows the dependence of peak current on sweep rate.

As shown from the Nyquist plot in Fig. 3B, the ohmic resistance of Ti_4O_7 was as low as that of the graphitic plate (3.8 Ω). Notably, the charge transfer resistance of Ti_4O_7 (20 Ω) was two orders of magnitude smaller than that for graphitic plate (1150 Ω), suggesting a much higher activity of Ti_4O_7. This observation is also supported by Tafel plots (Fig. 3C), illustrating that the exchange current density for Ti_4O_7 ($j_0 = 3.95 \times 10^{-3}$ mA cm^{-2}) was two orders of magnitude higher than that for graphitic plate ($j_0 = 2.16 \times 10^{-5}$ mA cm^{-2}). In addition, the porous apertures have larger surface area than bulk electrode, and much lower pH as result of water oxidation can be maintained within the micro-porous structure than bulk electrolyte. [20] The pH gradient at solid/liquid interface greatly enhances mass transfer during electrochemical reactions.

Apart from activity, the electrode stability is also of particular importance in the EO process. The stability and lifetime of Ti_4O_7 were assessed using electrochemical accelerated life-span tests by recording potential with respect to time under extreme and harsh conditions (3.0 mol L^{-1} H_2SO_4 and current density of 10^3 mA cm^{-2}, 30 °C). As shown in Fig. 3D, starting from the initial value of 3.5 V, the potential tended to ascend gradually (0–350 h), and then reached the critical point of 5.0 V followed by a steep elevation within the ongoing several hours. The deactivation of Ti_4O_7 can be attributed to collapse of its crystalline structure at long-time and extremely high current density. [29] In comparison, the graphite plate had a much shorter serving time of 80 h due to rapid electrochemical corrosion of carbon.

Based on the methods described by Hine et al. [24] the working life time (t_W) of electrode at a defined current density could be approximately estimated according to

$$\frac{t_W}{t_0} = \left(\frac{j_0}{j_W}\right)^n \quad (6)$$

where t_0 is the serving time at tested current density of $j_0 = 10^3$ mA cm^{-2}, j_W (mA cm^{-2}) the working current density commonly adopted in electrochemical oxidation and n the dimensionless number in the range of 1.4–2.0. Assuming a working current density j_W of 20 mA cm^{-2} and an n value of 1.7, an average lifetime of approximately 30 years is expected for Ti_4O_7, in contrast to 7 years for graphite plate. The Ti_4O_7 electrode outcompetes graphite electrode, and has a service lifetime on the same order of magnitude to Ti/Pt/IrO_x, [30] Ti/IrO_x and Ti/IrO_x-Sb_2O_5-SnO_2 [31,32]. The longevity and pronounced stability would be highly desired for wastewater treatment.

3.3. Electrocatalytic Oxidation of Industrial DFWW

Considering local discharge standard of 80 mgCOD L^{-1} regulated by Environment Protection Agency of China (GB 4287-2012), we evaluated the performances of monolithic Ti_4O_7 anode for EO removal of organic pollutants in industrial DFWW without any addition of chemical agents. Visual inspection shows that the dark-yellow wastewater changed rapidly to a clear and transparent solution (Fig. S3), demonstrating the effectiveness of Ti_4O_7 for treating DFWW. As illustrated in Fig. 4A and B, the greater removal of organic pollutants was achieved at longer reaction time and higher current density. With increased current density in the range of 2–30 mA cm^{-2}, the final COD and DOC in the treated effluent was decreased from 113.5 mg L^{-1} (39.4%) to 55.7 mg L^{-1} (70.2%), and

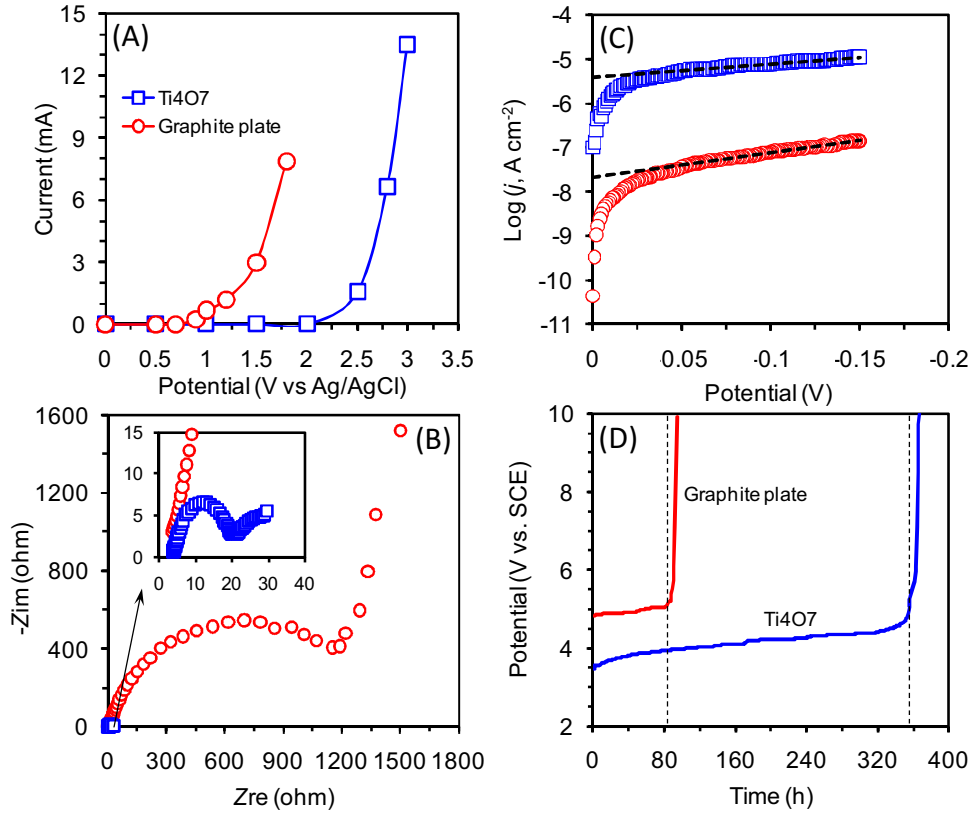

Fig. 3. (A) Amperometric measurement at different potentials, (B) Nyquist plot and (C) Tafel plot of monolithic Ti_4O_7 and graphite plate electrode obtained in 0.5 mol L^{-1} Na_2SO_4 electrolyte. (D) Time course of potential during accelerated life tests in 3.0 mol L^{-1} H_2SO_4 at current density of 10^3 mA cm^{-2} and temperature of 30 °C.

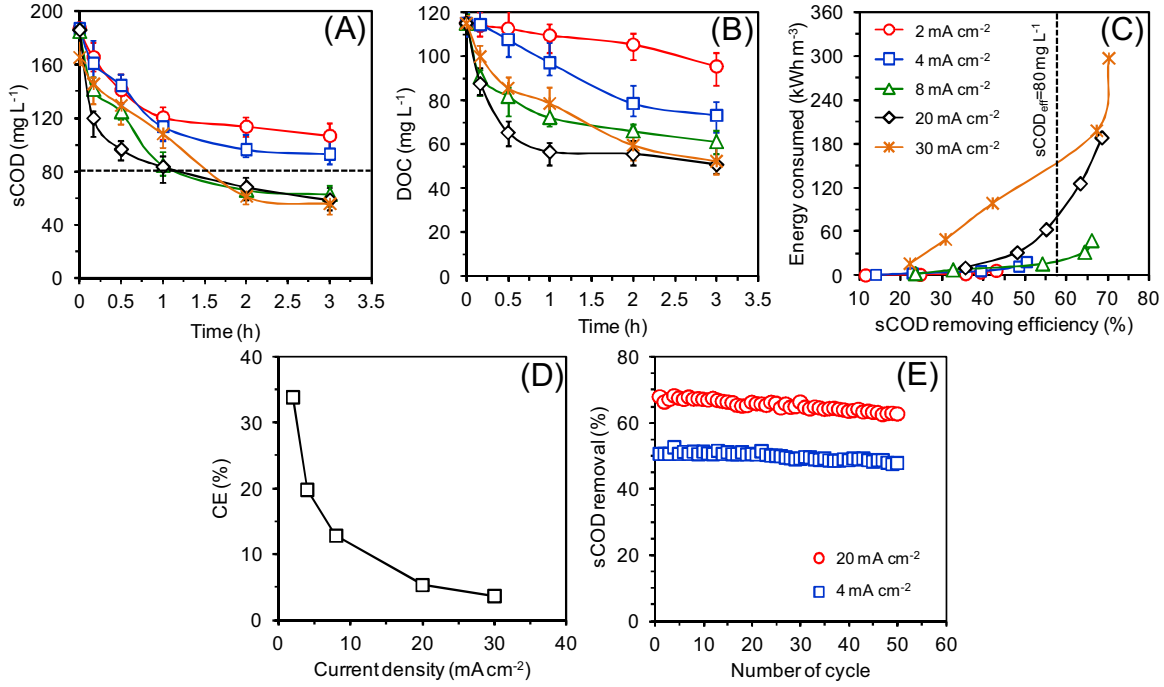

Fig. 4. Removal of (A) COD and (B) DOC as function of reaction time, (C) energy consumed with respect to COD removing efficiency and current density, (D) CE as function of current density, and (E) COD removal (2 h) during 50-cycle experiments.

from 105.3 mg L^{-1} (8.5%) to 52.3 mg L^{-1} (54.5%), respectively. This is due to more charge entailed passing the electrode for producing active species (*e.g.* •OH and active chlorine). [33] Meanwhile, the energy consumption was also increased, particularly for the current density in excess of 20 mA cm^{-2} (Fig. 4C). It was noticed that further increasing current density to 20–30 mA cm^{-2} and electrolysis time did not contribute significant improvement of COD removal. Instead, it caused sharp CE decline and far more energy consumption, which is attributed to the emergence of mass transport limitation and parasite reactions such as oxygen evolution reaction at higher current density. Based on the compromise between organic removal and energy consumption, the COD removal was optimized at current density of 8 mA cm^{-2} and reaction time of 2 h, which corresponded to overall removal efficiency of 68.8% (58.5 mg L^{-1} in the effluent), current efficiency (CE) of 12.8% (Fig. 4D), and energy consumption of 32 kWh m^{-3}. This combination of current density and treatment time appears to be much lower than that commonly practiced for electrolysis, implying significant energy savings as well as minimized generation of EO byproducts such as ClO_2^-, ClO_3^-, ClO_4^-, organic halogen (AOX), and trihalomethanes (THMs) [34,35].

The EO treatment increased the BOD_5/COD ratio by one order of magnitude (from initial 0.029 to 0.28) along with organic removal, suggesting a considerable improvement of the bioavailability of the treated effluent (Fig. S4). As revealed in HPLC-ESI/MS analysis, the electrochemical oxidation led to the decrease and even disappearance of most characteristic $\pm m/z$ peaks within a broad range of spectra, particularly for those with intensity of 10–40 and m/z of 160–340 (Fig. 5 and Table S2). The decomposition of these organic molecules is likely responsible for the improved bioavailability of EO-treated effluent.

The long-term stability of Ti_4O_7 for abatement of COD was investigated under current density of 4 mA cm^{-2} and 20 mA cm^{-2}. During a 50-cycle operation, the maximum COD removal declined by only 5.3% for 4 mA cm^{-2} and 7.7% for 20 mA cm^{-2}, respectively (Fig. 4E). These results clearly suggested a high corrosion resistance and good stability of Ti_4O_7 under anodic conditions, and the stable COD removal also accords well with the results from the accelerated life-span tests (Fig. 3D). The performance degradation under higher current density may be associated with the deactivation of outside surface of Ti_4O_7 thin film, leading to the formation of more oxidative titanium oxides [29].

3.4. Electrocatalytic Mechanisms

The electrochemical abatement of organic compounds can be related to direct oxidation and/or •OH-induced indirect oxidation on Ti_4O_7 electrode. [15,16] However, it seems far more complicated for the case of industrial wastewater, because the presence of high-concentration chloride ions inevitably overlaps the discharge of water and chloride at current density accompanying the anode potential available for both oxygen and chlorine evolution.

To minimize the side impact of impurities in industrial wastewater, NaCl solution (100 mg L^{-1}) was electrolyzed at current density of 2 mA cm^{-2} and 20 mA cm^{-2}, in order to qualitatively examine the formation of •OH on Ti_4O_7. The application of low current density allows for maximizing the extent to which water is oxidized by depressing subsidiary reactions induced by chlorides. Fig. 6A shows the typical response of DMPO-•OH adduct with quartet lines accounting for peak strength of 1:2:2:1 and hyperfine coupling constant of $_{\alpha N}$ = 1.49 mT and $_{\alpha H}$ = 1.49 mT (*g*-factor of 2.0055). The detectable DMPO-•OH was in good consistence with the observation of electrogenerated •OH on BDD. [36,37] It is further in line with Chen [38] who reported the EPR profiles of DMPO-•OH produced by Ti_4O_7 ceramics, and Zaky and Chaplin [15] who provided an indirect verification for the existence of •OH generated on Ti_4O_7 using *p*-benzoquinone as •OH probe. Taken together, the •OH-triggered organic decomposition on Ti_4O_7 can be described below:

$$H_2O + Ti_4O_7 \rightarrow [OH]_{ads} - Ti_4O_7 + H^+ + e^- \quad (7)$$

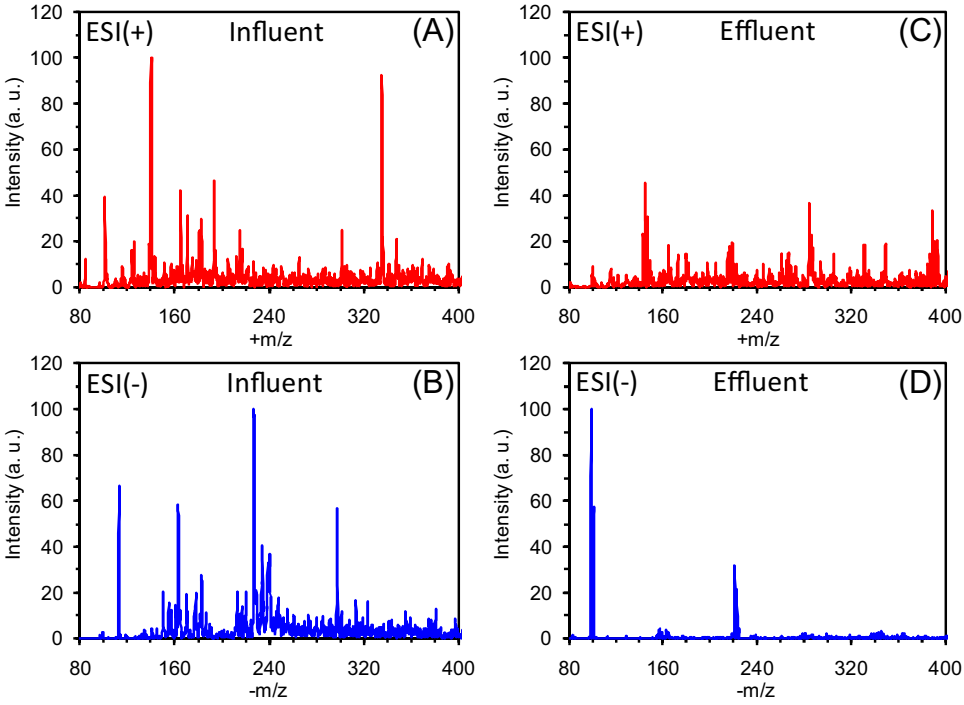

Fig. 5. HPLC-ESI/MS spectra for DFWW (A, B) and treated effluent (C, D) during electrocatalytic oxidation by monolithic Ti_4O_7 based on current density of 8 mA cm^{-2} and reaction time of 2 h.

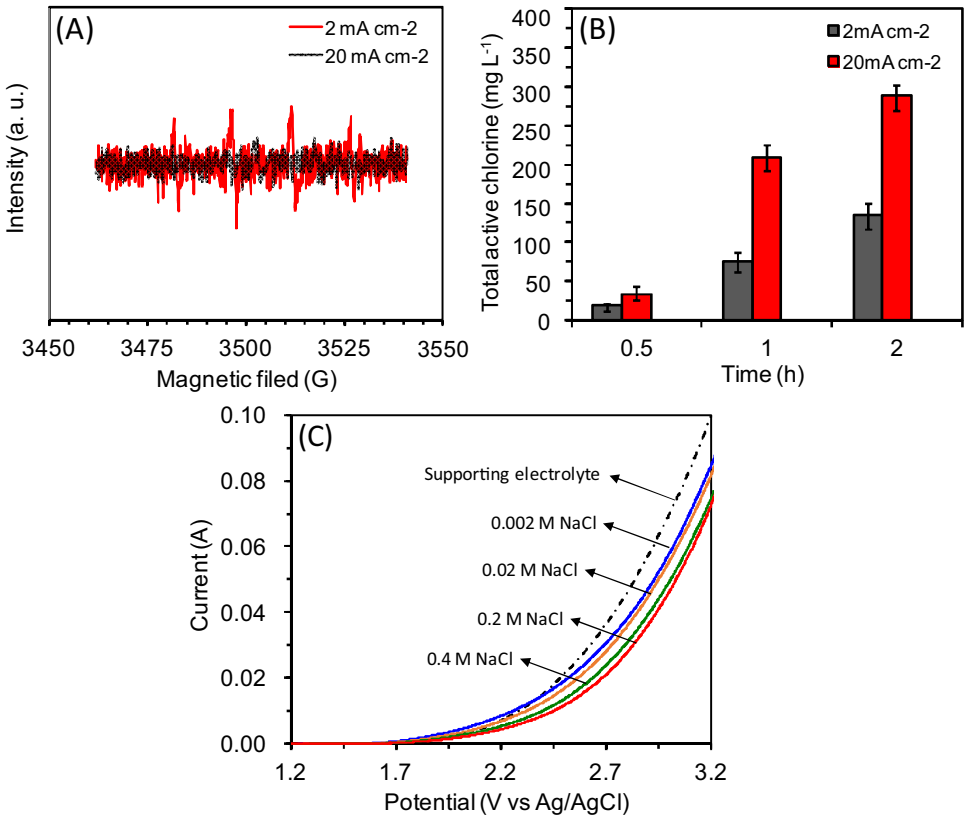

Fig. 6. (A) EPR spectra of DMPO-•OH adduct (reaction time of 2 h) and (B) total active chlorine at different current density. The electrolysis was performed in NaCl electrolyte (1000 mg L^{-1}, pH = 8.3). (C) The current-potential scan of the electrode in the presence of different concentration of NaCl with Na_2SO_4 (0.5 mol L^{-1}) electrolyte.

$$[OH]_{ads} - Ti_4O_7 + R \rightarrow Ti_4O_7 + CO_2 + H_2O + \text{Inorganic products} \quad (8)$$

$$[OH]_{ads} + [OH]_{ads} \rightarrow [H_2O_2]_{ads} \rightleftharpoons [H_2O_2]_{aq} \rightarrow H_2O + O_2 \quad (9)$$

Bejan et al. [39] reported the ability of Ti_4O_7 to produce •OH in a manner being similar as that of BDD. According to these authors, the Ti_4O_7 bounds •OH is more loosely and less abundantly in physisorbed state, and is more reactive than BDD. Because of such nature, the dimerization of •OH is more likely to proceed with the formation of H_2O_2 (Eq. (9)), which constitutes one possible explanation to the reason why a relatively low current efficiency is attained here for Ti_4O_7.

The total chlorine was found to increase more considerably at high current density than that at low current density (Fig. 6B). Meanwhile, the characteristic peaks for DMPO-•OH adduct faded in EPR spectra as a consequence of suppression by Cl^- oxidation when mass transfer predominates at high current density. It gives rise to a possible alternative mechanism that the •OH reacts with Cl^- to from physisorbed $^{\bullet}ClOH^-$ and consecutive HClO [40–44]. As can be seen in Fig. 6C, with the increase in chloride concentration, the polarization curves were shifted to more positive region; while increasing chloride concentration to 0.2 mol L^{-1} resulted in the reversal of the curves, indicating the importance of Cl_2/H_2O system as a potentiostatic buffer [45,46].

For the slightly alkaline DFWW (pH 8.38), the generated active chlorine in the form of ClO^- (pK_a of 7.44) may be responsible for abatement of organic compounds (R) in aqueous solution: [47]

$$2Cl^- + Ti_4O_7 \rightarrow 2e^- + [Cl_2]_{ads} - Ti_4O_7 \rightleftharpoons [Cl_2]_{aq} + Ti_4O_7 \quad (10)$$

$$Cl_2 + H_2O \rightleftharpoons Cl^- + H^+ + HClO \rightleftharpoons ClO^- + H^+ \quad (11)$$

$$Cl^- + [OH]_{ads} - Ti_4O_7 \rightarrow [ClOH^-]_{ads} - Ti_4O_7 \rightleftharpoons [HClO]_{ads} + Ti_4O_7 + e^- \quad (12)$$

$$HClO + 2H^+ + R(2e^-) \rightarrow CO_2 + H_2O + Cl^- + \text{inorganic products} (E^0 = +1.72\ V) \quad (13)$$

$$ClO^- + 2H_2O + R(2e^-) \rightarrow CO_2 + 2OH^- + Cl^- + \text{inorganic products} (E^0 = +0.89\ V) \quad (14)$$

This analysis was consistent with the observation of temporal increase in pH value during each cycle of anodic oxidation, especially at higher current density (Fig. S5). The reaction (14) represents a very significant pathway of indirect electro-oxidation for chloride-containing wastewater as extensively studied in previous works [48,49]. Besides, the possibility of physisorbed HClO shown in Eq. (12) may not be excluded, though the electrolyte is alkaline. This can be understood from the micro-scale porous structure of Ti_4O_7. The water oxidation at the anode results in acidification of electrolyte being adjacent to electrode surface (Eq. (7)). The Ti_4O_7 electrode can preserve much lower pH inside the porous structure than in bulk solution, thereby a substantial pH gradient is created between anode surface and bulk solution, thus favoring enhanced chloride oxidation [20–23].

Combing the above analysis and experimental results, the Ti_4O_7 should proceed with electrochemical oxidation of organic pollutants in industrial DFWW by active species of physisorbed •OH and HClO, and aqueous ClO^- under mass transfer control condition. ICE was decreased greatly with the increased current density (Fig. S6), due to heat dissipation and coulombic loss toward undesired side reactions. These reactions may include, but not limited to, dimerization of •OH, consecutive oxidation of ClO_2^-, ClO_3^-, ClO_4^-, organic halogen (AOX), and trihalomethanes (THMs), as well as cathodic reduction of oxidative species by electrons and produced H_2 [50]. In addition to decrease in treating efficiency, the concern should be also stressed on the behaviors of these toxic chlorinated byproducts in the treated effluent, which will be an important issue to be further addressed in the future studies.

3.5. Applications and Implications

The feasibility of monolithic porous Ti_4O_7 for tertiary treatment of DFWW is demonstrated in this study. The Ti_4O_7 can achieve efficient decomposition of organic substances upon energy consumption of 32 kWh m^{-3}, accounting for overall removing efficiency of 66.5% of COD and 46.7% of DOC at current density of 8 mA cm^{-2} and reaction time of 2 h. The quality of treated stream meets the discharge standard issued by EPA of China. The bioavailability of wastewater was improved greatly, represented by increase in BOD_5/COD ratio from initial 0.029 to 0.28. This means also implies that the treated effluent can be recirculated back to bio-process to further enhance the organic removal efficiency.

Table 1 gives a comparison of real industrial dyeing wastewater treatment by EO. Graphite, Ti/Pt, Ti/metal-doping oxides, dimensionally stable anode (DSA) and BDD could remove organic pollutants with efficiency in the range of 25-99% depending on initial COD or TOC, but these results were obtained mostly either by actively adding chemicals to adjust solution properties (*e.g.* pH and conductivity) or by applying high current density (28–100 mA cm^{-2}) with great energy consumption. In comparison, Ti_4O_7 demonstrated more superior performances at a much lower current density of 8 mA cm^{-2} without extra addition of chemicals. In the light of above results, Ti_4O_7 may become a promising candidate electrode material, whose unique properties make it more cost effective than BDD, and more environmentally friendly than PbO_2- and SnO_2-based electrodes. First, as a non-active electrode material, Ti_4O_7 has good conductivity and excellent stability approaching that of ceramic. The oxygen evolution potential as high as 2.5 V allows for water oxidation to produce •OH radicals before oxygen evolution. This property would be highly desirable to promote efficiency and selectivity of organic oxidation, which is virtually desired for wastewater treatment. Second, a major attraction of Ti_4O_7 is that it can be produced from TiO_2, a commodity chemical that are readily available and environmentally friendly across the world. This would render the electrode preparation and operation process more economically reliable and more sustainable. Third, the monolithic electrode is preferred for practical applications, because it eliminates the requirement for binding particulate catalyst onto conductive substrate during electrode fabrication. Thus, improvement of electrode stability is expected owing to minimal concern of particle agglomeration and detachment during long-term operation. As Heyfield marked, "It is fair to assert that in its combination of properties, monolithic Ti_4O_7 has no challengers" [9].

Notwithstanding this, there remains a long distance from what can be expected of Ti_4O_7 as an "ideal" electrode material for EO process, and several problems will continue to be further addressed. The future works may be more focused on several aspects, *e.g.* developing reliable methods for large-scale preparation of pure phase Ti_4O_7, designing suitable microporous structure for enhancing interfacial reaction, inhibiting side reactions to minimize chlorinated byproducts, constructing optimum Ti_4O_7-oriented configuration of electrochemical reactors. Additionally, it will be also of great interest to develop theoretical approaches like density functional theory to elucidate interaction between Ti_4O_7 and •OH radicals.

4. Conclusions

In this study, a monolithic porous Magnéli-phase Ti_4O_7 electrode was fabricated for electrochemical oxidation of refractory industrial DFWW. The Ti_4O_7 electrode achieved efficient and stable abatement of recalcitrant organic pollutants without any extra addition of chemicals. The soluble chemical oxygen demand (COD) and dissolved organic carbon (DOC) were removed by 66.5%

Table 1
Comparison of EO performances of treating real industrial dyeing wastewater.

Electrode	Experimental conditions		j (mA cm^{-2})	Time (h)	Removal (%)	Energy consumption	Refs.
	Initial COD (mg L^{-1})	Electrolyte					
Graphite rod	COD = 20840	pH 1.3	28	3.5	68	N. A. [b]	[51]
Graphite	COD = 347	0.5 mol L^{-1} NaCl, pH = 5.5	111.11	2	91.07	190 kWh kg COD^{-1}	[52]
Ti/Pt	COD = 608	pH = 7.0	12 V [a]	1.25	45	1800 kWh kg COD^{-1}	[53]
Ti/Pt	COD = 1250	1% NaCl	N. A.	1/6	90	N. A.	[54]
$Ti/Ru_{0.3}Ti_{0.7}O_2$	TOC = 225	5.85 g L^{-1} NaCl, Na_2SO_4, pH = 6.9	160	2	57.8	822 kWh kg TOC^{-1}	[55]
$Ti/Ru_{0.1}Sn_{0.9}O_2$	TOC = 225	0.1 mol L^{-1} NaCl, pH = 6.9	40	2	25.3	327 kWh kg TOC^{-1}	[56]
$Ti/Ru_{0.2}Sn_{0.8}O_2$					26.8	287 kWh kg TOC^{-1}	
$Ti/Ru_{0.3}Sn_{0.7}O_2$					23.9	325 kWh kg TOC^{-1}	
$Ti/Ir_{0.3}Ti_{0.7}O_2$					25.1	352 kWh kg TOC^{-1}	
$Ti/Ru_{0.3}Ti_{0.7}O_2$					44.4	159 kWh kg TOC^{-1}	
Ti-Pt/β-PbO_2	COD = 550	0.1 mol L^{-1} Na_2SO_4, pH = 7.0	75	3	90	50 kWh m^{-3}	[57]
DSA					55	31 kWh m^{-3}	
DSA	COD = 5957	16.7% NaCl, pH = 7.3	99.7	0.3	52.8	N. A.	[58]
Ti/RuO_xTiO_x	COD = 5400	pH = 8.0	40	5	95	24.95 kWh kg COD^{-1}	[59]
BDD	COD = 470	0.25 mol L^{-1} $HClO_4$, pH = 1.0	8	3	60	115 kWh kg COD^{-1}	[60]
BDD	COD = 650	5.0 g Na_2SO_4, pH = 10.0	60	15	99	300 kWh m^{-3}	[61]
Nb/BDD	COD = 300	0.1 mol L^{-1} Na_2SO_4, pH = 7.1	5	5	93	30 kWh m^{-3}	[62]
Monolithic porous Ti_4O_7	COD = 187.2 DOC = 108.5	No adjustment	8	2	68.8 (COD) 54.5 (DOC)	32 kWh m^{-3}	this work

[a] The electrolysis was carried out under potential control rather than current control.
[b] Data not reported.

and 46.7%, respectively, at current density of 8 mA cm^{-2} after 2 h reaction. The bioavailability of treated wastewater was improved substantially, indicated by one order of magnitude increase in BOD_5/COD. The Ti_4O_7 electrode had good long-term stability, with its maximum COD removal declined only slightly (<8%) at current density of 20 mA cm^{-2} during a 50-cycle operation. This study provides important insights for achieving efficient and sustainable electrochemical wastewater treatment using the novel porous Ti_4O_7 electrode material.

Acknowledgements

Project supported by the National Natural Science Foundation of China (No. 51378143, 51678184), State Key Laboratory of Urban Water Resource and Environment (Grant No. 2015TS01), the Fundamental Research Funds for the Central Universities (Grant No. HIT.BRETIII.201419). Many thanks go to Mr. Jian Li (Shanghai) for providing wastewater samples during the course of this study.

Appendix A. Supplementary data

Supplementary data associated with this article can be found, in the online version, at http://dx.doi.org/10.1016/j.electacta.2016.08.037.

References

[1] C.A. Martínez-Huitle, M.A. Rodrigo, I. Sires, O. Scialdone, Single and coupled electrochemical processes and reactors for the abatement of organic water pollutants: a critical review, Chem. Rev. 115 (2015) 13362–13407.
[2] B.P. Chaplin, Critical review of electrochemical advanced oxidation processes for water treatment applications, Environ. Sci. Processes Impacts 16 (2014) 1182–1203.
[3] X. Li, D. Pletcher, F.C. Walsh, Electrodeposited lead dioxide coatings, Chem. Soc. Rev. 40 (2011) 3879–3894.
[4] H. Chang, D.C. Johnson, Electrocatalysis of anodic oxygen-transfer reactions ultrathin films of lead oxide on solid electrodes, J. Electrochem. Soc. 137 (1990) 3108–3113.
[5] A. Kapałka, G. Fóti, C. Comninellis, The importance of electrode material in environmental electrochemistry: Formation and reactivity of free hydroxyl radicals on boron-doped diamond electrodes, Electrochim. Acta 54 (2009) 2018–2023.
[6] X. Zhu, M. Tong, S. Shi, H. Zhao, J. Ni, Essential explanation of the strong mineralization performance of boron-doped diamond electrodes, Environ. Sci. Technol. 42 (2008) 4914–4920.
[7] X. Yu, M. Zhou, Y. Hu, K. Groenen-Serrano, F. Yu, Recent updates on electrochemical degradation of bio-refractory organic pollutants using BDD anode: a mini review, Environ. Sci. Pollut. Res. 21 (2014) 8417–8431.
[8] S. Garcia-Segura, E.V. dos Santos, C.A. Martínez-Huitle, Role of sp3/sp2 ratio on the electrocatalytic properties of boron-doped diamond electrodes: A mini review, Electrochem. Commun. 59 (2015) 52–55.
[9] P.C.S. Hayfield, Development of a new material-monolithic Ti_4O_7 Ebonex® ceramic, Royal Society of Chemistry, Cambridge, U.K, 2002.
[10] A.C.M. Padilha, J.M. Osorio-Guillén, A.R. Rocha, G.M. Dalpian, Ti_nO_{2n-1} Magnéli phases studied using density functional theory, Phys. Rev. B. 90 (2014) 1–7.
[11] R.J. Pollock, Electrochemical properties of a new electrode material Ti_4O_7, Mater. Res. Bull. 19 (1984) 17–24.
[12] J.E. Graves, D. Pletcher, R.L. Clarke, F.C. Walsh, The electrochemistry of Magnéli phase titanium oxide ceramic electrodes Part I. The deposition and properties of metal coatings, J. Appl. Electrochem. 21 (1991) 848–857.
[13] F.C. Walsh, R.G.A. Wills, The continuing development of Magnéli phase titanium sub-oxides and Ebonex® electrodes, Electrochim. Acta 55 (2010) 6342–6351.
[14] A.E. Stoyanova, E.D. Lefterova, V.I. Nikolova, P.T. Iliev, I.D. Dragieva, E.P. Slavcheva, Water splitting in PEM electrolysis with Ebonex® supported catalysts, Bul. Chem. Commun. 42 (2010) 167–173.
[15] A.M. Zaky, B.P. Chaplin, Porous substoichiometric TiO_2 anodes as reactive electrochemical membranes for water treatment, Environ. Sci. Technol. 47 (2013) 6554–6563.
[16] A.M. Zaky, B.P. Chaplin, Mechanisms of *p*-substituted phenol oxidation at a Ti_4O_7 reactive electrochemical membrane, Environ. Sci. Technol. 48 (2014) 5857–5867.
[17] P. Geng, J. Su, C. Miles, C. Comninellis, G. Chen, Highly-ordered Magnéli Ti_4O_7 nanotube arrays as effective anodic material for electro-oxidation, Electrochim. Acta 153 (2015) 316–324.
[18] K. Sarayu, S. Sandhya, Current technologies for biological treatment of textile wastewater-A review, Appl. Biochem Biotechnol. 167 (2012) 645–661.
[19] Discharge standards of water pollutants for dyeing and finishing of textile industry GB 4287-2012, Environment Protection Agency of China, 2012.12.19.
[20] C. Tan, B. Xiang, Y. Li, J. Fang, M. Huang, Preparation and characteristics of a nano-PbO_2 anode for organic wastewater treatment, Chem. Eng. J. 166 (2011) 15–21.
[21] D. Ghernaout, M. Wahib Naceur, A. Aouabed, On the dependence of chlorine by-products generated species formation of the electrode material and applied charge during electrochemical water treatment, Desalination 270 (2011) 9–22.
[22] O. Scialdone, S. Randazzo, A. Galia, G. Silvestri, Electro-chemical oxidation of organics in water: role of operative parameters in the absence and in the presence of NaCl, Water Res. 43 (2009) 2260–2272.
[23] S. Trasatti, Progress in the Understanding of the mechanism of chlorine evolution at oxide electrodes, Electrochim. Acta 32 (1987) 369–382.
[24] F. Hine, M. Yasuda, T. Noda, T. Yoshida, J. Okuda, Electrochemical behavior of the oxide-coated metal anodes, J. Electrochem. Soc. 126 (1979) 1439–1445.
[25] American Public Health Association, American Water Works Association, Water Pollution Control Federation, standard methods for the examination of water and wastewater, 18th ed., American Public Health Association, Washington, DC, 1995.
[26] D. Regonini, A.C.E. Dent, C.R. Bowen, S.R. Pennock, J. Taylor, Impedance spectroscopy analysis of Ti_nO_{2n-1} Magnéli phases, Mater. Lett. 65 (2011) 3590–3592.
[27] A.A. Gusev, E.G. Avvakumov, A.Z. Medvedev, A.I. Masliy, Ceramic electrodes based on Magnéli phases of titanium oxides, Sci. Sinter. 39 (2007) 51–57.
[28] S. Levine, A.L. Smith, Theory of the differential capacity of the oxide/aqueous electrolyte interface, Discuss. Faraday Soc. 52 (1971) 290–301.
[29] J.R. Smith, F.C. Walsh, R.L. Clarke, Electrodes based on Magneli phase titanium oxides: the properties and applications of Ebonex® materials, J. Appl. Electrochem. 28 (1998) 1021–1033.
[30] R. Hutchings, K. Muller, F. Kotz, K.S. Stucki, A structural investigation of stabilized oxygen evolution catalysts, J. Mater. Sci. 12 (1984) 3987–3994.
[31] X.M. Chen, G.H. Chen, P.L. Yue, Novel electrode system for electroflotation of wastewater, Environ. Sci. Technol. 36 (2002) 778–783.
[32] X. Chen, G. Chen, P.L. Yue, Stable Ti/IrO_x-Sb_2O_5-SnO_2 anode for O_2 evolution with low Ir content, J. Phys. Chem. B 105 (2001) 4623–4628.
[33] N. Mohan, N. Balasubramanian, C.A. Bash, Electrochemical oxidation of textile wastewater and its reuse, J. Hazard. Mater. 147 (2007) 6444–6651.
[34] A.Y. Bagastyo, D.J. Batstone, I. Kristiana, W. Gernjak, C. Joll, J. Radjenovic, Electrochemical oxidation of reverse osmosis concentrate on boron-doped diamond anodes at circumneutral and acidic pH, Water Res. 46 (2012) 6104–6112.
[35] V. Schmalz, T. Dittmar, D. Haaken, E. Worch, Electrochemical disinfection of biologically treated wastewater from small treatment systems by using boron-doped diamond (BDD) electrodes-Contribution for direct reuse of domestic wastewater, Water Res. 43 (2009) 5260–5266.
[36] B. Marselli, J. García-Gomez, P.A. Michaud, M.A. Rodrigo, C. Comninellis, Electrogeneration of hydroxyl radicals on boron-doped diamond electrodes, J. Electrochem. Soc. 150 (2003) D79–D83.
[37] M. Panizza, G. Fóti, L. Guo, X. Li, G. Chen, in: C. Comninellis, G. Chen (Eds.), Electrochemistry for the Environment, Springer, New York, 2010 Chapter 2.
[38] G.S. Chen, Electrochemical and thermochemical destruction of chlorinated solvents. Ph. D, Dissertation, The University of Arizona, U.S, 2000 UMI No.: 9972125.
[39] D. Bejan, E. Guinea, N.J. Bunce, On the nature of the hydroxyl radicals produced at boron-doped diamond and Ebonex® anodes, Electrochim. Acta 69 (2012) 275–281.
[40] L. Szpyrkowicz, J. Naumczykt, F. Zilio-Grandi, Application of electrochemical processes for tannery wastewater treatment, Toxicol. Environ. Chem. 44 (1994) 189–202.
[41] F. Bonfatti, S. Ferro, F. Lavezzo, M. Malacarne, G. Lodi, A. De Battisti, Electrochemical incineration of glucose as a model organic substrate II. role of active chlorine mediation, J. Electrochem. Soc. 147 (2000) 592–596.
[42] I. Sirés, E. Brillas, M.A. Oturan, M.A. Rodrigo, M. Panizza, Electrochemical advanced oxidation processes: today and tomorrow. A review, Environ. Sci. Pollut. Res. 21 (2014) 8336–8367.
[43] C.A. Martínez-Huitle, E. Brillas, Electrochemical alternatives for drinking water disinfection, Angew. Chem. Int. Ed. 11 (2008) 1998–2005.
[44] E. Brillas, C.A. Martínez-Huitle, Decontamination of wastewaters containing synthetic organic dyes by electrochemical methods. An updated review, Appl. Catal. B: Environ. 166–167 (2015) 603–643.
[45] J.H. Bezerra Rocha, M.M. Soares Gomes, E. Vieira dos Santos, E.C. Martins de Moura, D. Ribeiro da Silva, M.A. Quiroz, C.A. Martínez-Huitle, Electrochemical degradation of Novacron Yellow C-RG using boron-doped diamond and platinum anodes: Direct and Indirect oxidation, Electrochim. Acta 140 (2014) 419–426.
[46] C.A. Martínez-Huitle, S. Ferro, A. De Battisti, Electrochemical incineration in the presence of halides, Electrochem. Solid-State Lett. 8 (2005) D35.
[47] C.A. Martínez-Huitle, E. Brillas, Decontamination of wastewaters containing synthetic organic dyes by electrochemical methods: A general review, Appl. Catal. B-Environ. 87 (2009) 105–145.
[48] C.A. Martínez-Huitle, S. Ferro, Electrochemical oxidation of organic pollutants for the wastewater treatment: direct and indirect processes, Chem. Soc. Rev. 35 (2006) 1324–1340.
[49] M. Panizza, G. Cerisola, Direct and mediated anodic oxidation of organic pollutants, Chem. Rev. 109 (2009) 6541–6569.

[50] M.E.H. Bergmann, J. Rollin, Product and by-product formation in laboratory studies on disinfection electrolysis of water using boron-doped diamond anodes, Catal. Today 124 (2007) 198–203.
[51] K.V. Radha, V. Sridevi, K. Kalaivani, Electrochemical oxidation for the treatment of textile industry wastewater, Bioresour. Technol. 100 (2009) 987–990.
[52] R. Bhatnagar, H. Joshi, I.D. Mall, V.C. Srivastava, Electrochemical oxidation of textile industry wastewater by graphite electrodes, J. Environ. Sci. Heal Part A 49 (2014) 955–966.
[53] A. Sakalis, K. Mpoulmpasakos, U. Nickel, K. Fytianos, A. Voulgaropoulos, Evaluation of a novel electrochemical pilot plant process for azodyes removal from textile wastewater, Chem. Eng. J. 111 (2005) 63–70.
[54] A.G. Vlyssides, D. Papaioannou, M. Loizidoy, P.K. Karlis, A.A. Zorpas, Testing an electrochemical method for treatment of textile dye wastewater, Waste Manage. 20 (2000) 569–574.
[55] G.R. Malpass, D.W. Miwa, D.A. Mortari, S.A. Machado, A.J. Motheo, Decolorisation of real textile waste using electrochemical techniques: effect of the chloride concentration, Water Res. 41 (2007) 2969–2977.
[56] G.R. Malpass, D.W. Miwa, S.A. Machado, A.J. Motheo, Decolourisation of real textile waste using electrochemical techniques: effect of electrode composition, J. Hazard. Mater. 156 (2008) 170–177.
[57] J.M. Aquino, R.C. Rocha-Filho, L.A.M. Ruotolo, N. Bocchi, S.R. Biaggio, Electrochemical degradation of a real textile wastewater using β-PbO_2 and DSA® anodes, Chem. Eng. J. 251 (2014) 138–145.
[58] S.S. Vaghela, A.D. Jethva, B.B. Mehta, S.P. Dave, S. Adimurthy, G. Ramachandraiah, Laboratory studies of electrochemical treatment of industrial azo dye effluent, Environ. Sci. Technol. 39 (2005) 2848–2855.
[59] J. Sendhil, P. Muniswaran, C. Ahmed Basha, Real textile dye wastewater treatment by electrochemical oxidation: Application of response surface methodology (Rsm), Int. J. Chem. Tech. Res. 7 (2014) 2681–2690.
[60] E. Tsantaki, T. Velegraki, A. Katsaounis, D. Mantzavinos, Anodic oxidation of textile dyehouse effluents on boron-doped diamond electrode, J. Hazard. Mater. 207–208 (2012) 91–96.
[61] C.A. Martínez-Huitle, E.V.D. Santos, D.M.D. Araújo, M. Panizza, Applicability of diamond electrode/anode to the electrochemical treatment of a real textile effluent, J. Electroanalytical. Chem. 674 (2012) 103–107.
[62] J.M. Aquino, G.F. Pereira, R.C. Rocha-Filho, N. Bocchi, S.R. Biaggio, Electrochemical degradation of a real textile effluent using boron-doped diamond or β-PbO_2 as anode, J. Hazard. Mater. 192 (2011) 1275–1282.